Modulation of Cardiac Troponin C−Cardiac Troponin I Regulatory Interactions by the Amino-terminus of Cardiac Troponin I†

M. Bret Abbott,‡ Wen-Ji Dong,§ Alex Dvoretsky,‡ Beverly DaGue,|| Richard M. Caprioli,|| Herbert C. Cheung,*,§ and Paul R. Rosevear*,‡

Department of Molecular Genetics, Biochemistry, and Microbiology, College of Medicine, University of Cincinnati, Cincinnati, Ohio 45267, Department of Biochemistry and Molecular Genetics, University of Alabama at Birmingham, Birmingham, Alabama 35294, and Mass Spectrometry Research Center, Vanderbilt University Medical Center, Nashville, Tennessee 37232-6400

Received January 9, 2001; Revised Manuscript Received March 15, 2001

ABSTRACT: Multidimensional heteronuclear magnetic resonance studies of the cardiac troponin C/troponin I(1−80)/troponin I(129−166) complex demonstrated that cardiac troponin I(129−166), corresponding to the adjacent inhibitory and regulatory regions, interacts with and induces an opening of the cardiac troponin C regulatory domain. Chemical shift perturbation mapping and ^{15}N transverse relaxation rates for intact cardiac troponin C bound to either cardiac troponin I(1−80)/troponin I(129−166) or troponin I(1−167) suggested that troponin I residues 81−128 do not interact strongly with troponin C but likely serve to modulate the interaction of troponin I(129−166) with the cardiac troponin C regulatory domain. Chemical shift perturbations due to troponin I(129−166) binding the cardiac troponin C/troponin I(1−80) complex correlate with partial opening of the cardiac troponin C regulatory domain previously demonstrated by distance measurements using fluorescence methodologies. Fluorescence emission from cardiac troponin $C(F20W/N51C)_{AEDANS}$ complexed to cardiac troponin I(1−80) was used to monitor binding of cardiac troponin I(129−166) to the regulatory domain of cardiac troponin C. The apparent K_d for cardiac troponin I(129−166) binding to cardiac troponin C/troponin I(1−80) was 43.3 ± 3.2 μM. After bisphosphorylation of cardiac troponin I(1−80) the apparent K_d increased to 59.1 ± 1.3 μM. Thus, phosphorylation of the cardiac-specific N-terminus of troponin I reduces the apparent binding affinity of the regulatory domain of cardiac troponin C for cardiac troponin I(129−166) and provides further evidence for β-adrenergic modulation of troponin Ca^{2+} sensitivity through a direct interaction between the cardiac-specific amino-terminus of troponin I and the cardiac troponin C regulatory domain.

Calcium binding to the troponin C (TnC)[1] subunit of the troponin complex is the initiating event that releases thin filament inhibition of striated muscle contraction. Upon Ca^{2+} binding, cTnC binds cTnI with high specificity and the cTnI inhibitory region no longer interacts with actin (*1*). Subsequent adjustments in troponin T (TnT), tropomyosin, and actin result in productive, force-generating interactions between the myosin head of the thick filament and actin in the thin filament.

TnC consists of two compact globular domains connected by the D/E linker (*2*). The C-domain of both skeletal and cardiac isoforms contains two EF-hand motifs that each bind Ca^{2+} or Mg^{2+} with high affinity (*3*). The N-domain, or regulatory domain, also contains two EF-hand motifs. However, these sites are Ca^{2+}-specific and have weaker affinity than the C-domain sites. Ca^{2+} binding site I of cardiac TnC (cTnC) is inactive due to two nonconservative substitutions and a single amino acid insertion, resulting in decreased cooperativity of force development. Upon Ca^{2+} binding to the skeletal TnC (sTnC) regulatory sites, the B- and C-helices

† This work supported by Grants AR 44324 (to P.R.R.) and HL52508 (to H.C.C.) and GM 58008 (to R.M.C.) from the National Institutes of Health.

‡ University of Cincinnati.

§ University of Alabama at Birmingham.

|| Vanderbilt University Medical Center.

* Authors to whom correspondence should be addressed. P.R.R.: Department of Molecular Genetics, Biochemistry, and Microbiology, University of Cincinnati, 231 Bethesda Ave., Room 2106A-MSB, Cincinnati, OH 45267-0524. Tel (513) 558-3370; fax (513) 555-8474; e-mail rosevear@proto.med.uc.edu. H.C.C.: 520 CH-19, Department of Biochemistry and Molecular Genetics, University of Alabama at Birmingham, Birmingham, AL 35294-2041. Tel (205) 934-2485; fax (205) 975-4621; e-mail hccheung@uab.edu.

[1] Abbreviations: TnC, troponin C; TnI, troponin I; TnT, troponin T; cTnC, recombinant cardiac troponin C (desMet[1]−Ala[2], Cys35Ser); sTnC, skeletal troponin C; cTnI, cardiac troponin I; cTnI(1−80), recombinant mouse cardiac troponin I corresponding to residues 2−80 with the N-terminal Met cleaved during expression; cTnI(1−80)pp, recombinant mouse cardiac troponin I residues 1−80 phosphorylated at Ser23 and Ser24; cTnI(1−167), recombinant mouse cardiac troponin I corresponding to residues 1−167; cTnI(129−166), synthetic peptide with sequence corresponding to mouse cardiac troponin I residues 129−166; DTT, dithiothreitol; IAEDANS, 5-(iodoacetamidoethyl)aminonaphthalene-1-sulfonic acid; $cTnC(F20W/N51C)_{AEDANS}$, recombinant cardiac troponin C with amino acid substitutions F20W and N51C covalently labeled with the 5-(iodoacetamidoethyl)aminonaphthalene-1-sulfonic acid fluorescent probe; PKA, cAMP-dependent protein kinase A; MOPS, 3-(*N*- morpholino)propanesulfonic acid; EGTA, ethylene glycol bis(β-aminoethyl ether)-*N*,*N*,*N*′,*N*′-tetraacetic acid; CPMG, Carr−Purcell−Meiboom−Gill; HSQC, heteronuclear single quantum coherence; NOESY, nuclear Overhauser enhancement spectroscopy; Tris, tris(hydroxymethyl)aminomethane; BCA, bicinchoninic acid; FRET, fluorescence resonance energy transfer.

10.1021/bi0100642 CCC: $20.00
Published on Web 04/26/2001

move away from the N-, A-, and D-helices, exposing the hydrophobic core of the domain (*4*−*7*). This conformation is referred to as the open state. However, in the cardiac system, due to the single Ca^{2+} binding site, interactions with the regulatory region of cTnI, as well as Ca^{2+} binding, are required to open the cTnC regulatory domain (*4, 5, 8, 9*). A dynamic equilibrium between open and closed conformations of Ca^{2+}-saturated cTnC has been proposed on the basis of evidence for rapid motions and conformational exchange in the cTnC regulatory domain (*10*−*12*).

TnI contains a number of regions of functional significance. The N-terminal region, corresponding to cTnI residues 37−70, binds tightly to the C-domain of TnC in a Ca^{2+}- and/or Mg^{2+}-dependent manner (*13*−*16*). This interaction tethers TnC to TnI throughout the contraction cycle. The inhibitory region, residues 129−147 of cTnI, inhibits muscle contraction via interactions with actin during the relaxation phase and may interact with cTnC near the D/E linker region during the contraction phase (*1, 17, 18*). The second TnC interaction site or regulatory region, corresponding to residues 147−166 of cTnI, interacts with the N-domain of cTnC in a calcium-dependent manner (*4, 9, 16*) and modulates the interactions between the cTnI inhibitory region and actin during the contraction cycle. The region of cTnI between residues 81−128 contains a heptad repeat motif often found in coiled-coil interactions and has been postulated to interact with cTnT (*19*).

PKA phosphorylation of the cardiac-specific N-terminus of cTnI reduces the apparent Ca^{2+}-binding affinity of cTnC site II in vitro and the Ca^{2+} sensitivity of force development in skinned fiber assays (*20*−*22*). Interactions between the nonphosphorylated cardiac-specific N-terminus of cTnI and the regulatory domain of cTnC are thought to favor the open conformation and stabilize interactions between the regulatory region of cTnI and the regulatory domain of cTnC (*12*). Interactions between the cardiac-specific cTnI N-terminus and the cTnC regulatory domain are lost upon PKA phosphorylation of the two adjacent cTnI serine residues at positions 23 and 24 (*10, 12*). The loss of these interactions could account for the reduced apparent Ca^{2+} binding affinity of cTnC in the presence of PKA phosphorylated cTnI. Taken together, these data suggest the hypothesis that PKA phosphorylation of the cardiac-specific N-terminus of cTnI alters the apparent strength of Ca^{2+}-dependent interactions between the regulatory domain of cTnC and the regulatory region of cTnI. Here we study the biochemical, structural, and dynamic consequences of PKA phosphorylation of the cardiac-specific N-terminus on the binding of the inhibitory and regulatory regions of cTnI to intact cTnC.

Heteronuclear multidimensional NMR was utilized to map cTnI(129−166) interactions to the regulatory domain of cTnC in the [^{15}N,^{2}H]cTnC/cTnI(1−80) complex. We have previously demonstrated partial structural opening of the regulatory domain by this peptide utilizing FRET methodologies and are now able to correlate a specific pattern of chemicals shift changes with this conformational change (*9*). Fluorescence emission from cTnC(F20/N51C)$_{AEDANS}$ was used to detect cTnI(129−166) interactions with the N-domain of cTnC in the absence of cTnI(1−80) and in the presence of unphosphorylated and PKA-phosphorylated cTnI(1−80). Dissociation constants indicated that phosphorylation of the cardiac-specific N-terminus of cTnI reduces the affinity of the cTnC regulatory domain for cTnI(129−166), resulting in altered cTnC regulatory domain conformational equilibria, providing a mechanism for phosphorylation-dependent alterations in the Ca^{2+} sensitivity of muscle contraction.

EXPERIMENTAL PROCEDURES (MATERIALS AND METHODS)

Proteins. cDNA encoding cTnI(1−167) was generated by PCR and subcloned into the pET23d^{+} expression vector. [^{15}N,^{2}H]cTnC, cTnI(1−80), and cTnI(1−167) were expressed and purified and complex formation was carried out as previously described (*10, 15, 23*). Electrospray mass spectrometry of purified cTnI(1−80) indicated cleavage of the N-terminal Met residue and identified no carbamylation or other protein modifications despite exposure of the protein to urea, PMSF, and other protease inhibitors during purification and sample preparation. Phosphorylation of cTnI(1−80) by PKA was carried out on a cTnC affinity column as previously described (*23, 24*). The extent of phosphorylation was better than 1.8 mol of phosphate/mol of peptide. For NMR experiments the [^{15}N,^{2}H]cTnC/cTnI(1−80) complex was prepared at 1.0 mM concentration in 10% $^{2}H_2O$, 20 mM Tris-d_{11} buffer (pH = 6.8), 150 mM potassium chloride, 10 mM Ca^{2+}, 5 mM DTT, and 1:1000 dilution of a protease inhibitor cocktail made by dissolving one tablet of Cømplete EDTA-free (Boehringer Mannheim, Germany) in 3 mL of MilliQ H_2O (*10, 23*). The Ca^{2+}-saturated [^{15}N,^{2}H]cTnC/cTnI(1−167) complex was prepared at 0.6 mM concentration in the same buffer. No evidence of cTnC dimerization or complex aggregation was observed by native gel electrophoresis or dynamic light scattering. Protein concentrations for cTnC were determined by UV and Bradford analysis. Cardiac TnI concentrations were determined by BCA assay (Pierce, Rockford, IL). Amino acid analysis of the cTnC/cTnI(1−80) complex was used to calibrate the Bradford protein assay. The peptide cTnI(129−166) (LTQKIYDLRGKFKRPTLRRVRISADAMMQALLGTRAKE) was synthesized and purified as a C-terminal amide as previously described (*9*). The peptide was quantitated by weight or amino acid analysis. During NMR titration experiments this peptide was added as a lyophilized powder to minimize dilution effects, and minor corrections in pH were made as necessary.

NMR Spectroscopy. All experiments were carried out on Varian 600 or 800 MHz spectrometers. ^{1}H−^{15}N correlation experiments utilized sensitivity-enhanced ^{1}H−^{15}N HSQC (*25*) based pulse sequences. Three-dimensional NOESY-HSQC experiments with 85 or 150 ms mixing times were generally used to confirm amide resonance assignments (*26*). Spectral widths in the t_1 and t_2 dimensions were 3.3 and 12 kHz, respectively. ^{15}N transverse relaxation rates were determined by use of a CPMG pulse sequence with relaxation periods of 0, 8, 16, 24, 32, 48, 64, 80, and 96 ms. Double points were collected with relaxation periods of 8 and 24 ms for error analysis. Data processing has been described previously (*10*). Composite amide chemical shift differences were determined from the square root of the weighted sum of the squares of proton and nitrogen chemical shift differences. ^{15}N chemical shift differences were weighted by a factor of $^{1}/_{7}$ to scale their contributions to a magnitude similar to ^{1}H chemical shift differences.

Fluorescence Spectroscopy. Steady-state fluorescence measurements were carried out at 20 ± 0.1 °C on a photon-counting ISS PC1 spectrofluorometer, using a band-pass of 3 nm for both excitation and emission wavelengths. Emission spectra were corrected for variation of the detector system with wavelength. Binding of the peptide cTnI(129−166) to the cTnC mutant (F20W/N51C)$_{AEDANS}$ in the presence of Ca^{2+} was determined by a method similar to that previously described (*9*). In a typical experiment, 2 μM of cTnC(F20W/N15C)$_{AEDANS}$ was titrated with cTnI(129−166) in a buffer containing 30 mM MOPS at pH 7.0, 0.3 M KCl, 0.5 mM DTT, 1 mM EGTA, 3 mM Mg^{2+}, and 2 mM Ca^{2+}. The concentration of the cTnI(1−80) domain was 20 μM when required. The fluorescence titration experiments were planned to make best use of limiting supplies of the costly cTnI(129−166) peptide. Experiments with large excesses of the cTnI(129−166) peptide were omitted in order to obtain replicate data points in the most relevant concentration range and to avoid confounding artifacts at excessive cTnI(129−166) concentrations. The changes in fluorescence intensity (F) of tryptophan in cTnC(F20W/N51C)$_{AEDANS}$ were used to determine the fraction of cTnI(129−166) that was bound to cTnC(F20W/N51C)$_{AEDANS}$:

$$Y = (F - F_0)/(F_\infty - F_0) \quad (1)$$

where F_0 is the initial fluorescence intensity of cTnC(F20W/N51C)$_{AEDANS}$ in the absence of cTnI(129−166) and F_∞ is the limiting intensity determined in the presence of excess cTnI(129−166). F_∞ was obtained from extrapolation of a plot of $1/(F - F_0)$ vs 1/[cTnI(129−166)]. The values of Y were then fitted to

$$Y = nK[x]/(1 + K[x]) \quad (2)$$

where K is the apparent binding constant, n is the number of binding sites, and [x] is the free cTnI(129−166) concentration. An iterative nonlinear least-squares procedure was used to estimate K and n.

RESULTS

To further explore the mechanism of cardiac muscle activation and modulation, we have studied binding of the cTnI inhibitory and regulatory regions to cTnC. The binary [^{15}N,^{2}H]cTnC/cTnI(1−80) complex was prepared and characterized as previously described (*23*). Electrospray mass spectroscopic analysis was used to ascertain the level of carbamylation present in cTnI(1−80). The extensive use of urea during purification of cTnI domains predisposes the proteins to carbamylation from trace amounts of cyanate present in concentrated urea solutions. Thus, mass spectroscopy was used to verify that all cTnI domains used in the experiments were greater than 90% free of carbamylate adducts. Structural perturbations in [^{15}N,^{2}H]cTnC bound to cTnI(1−80) upon titration with cTnI(129−166) were monitored in a series of ^{1}H−^{15}N HSQC spectra. Intact cTnC is required to study physiologically relevant interactions between cTnC and cTnI domains and the mechanism by which phosphorylation of cTnI modulates Ca^{2+}-binding affinity of the cTnC regulatory domain. Occupation of the cTnC C-domain hydrophobic pocket with the N-domain of cTnI not only modulates the conformation of the cTnC regulatory domain but also prevents artifactual cTnI peptide binding to the cTnC C-domain (*17*). This fact is borne out in a number of studies suggesting various conformations and cTnC binding sites for the cTnI inhibitory region (*4, 27*−*29*). The ^{1}H−^{15}N correlation spectrum of [^{15}N,^{2}H]cTnC/cTnI(1−80) has been assigned previously (*23*). Assignments for cTnC in the cTnC/cTnI(1−80)/cTnI(129−166) complex were made by carefully following chemical shift changes of [^{15}N,^{2}H]-cTnC bound to cTnI(1−80) through the titration with cTnI-(129−166). Assignments at a final cTnC/cTnI(1−80)/cTnI-(129−166) ratio of 1:1:2 were confirmed by sequential H_N to H_N NOEs observed in 85 and 150 ms NOESY-HSQC spectra. The ^{1}H−^{15}N HQSC spectrum of the cTnC/cTnI(1−80)/cTnI(129−166) complex at 800 MHz is provided in Figure 1A. Cross-peaks are labeled with resonance assignments. Chemical shift changes induced by binding of cTnI-(129−166) were confined to ^{1}H−^{15}N cross-peaks assigned to residues within the N-domain of cTnC. In a similar fashion, preliminary cross-peak assignments for [^{15}N,^{2}H]-cTnC bound to cTnI(1−167) were made by comparison with spectra of cTnC bound to cTnI(1−211) and confirmed by identification of sequential H_N to H_N NOEs observed in an 85 ms NOESY-HSQC spectrum (data not shown). A representative ^{1}H−^{15}N HSQC spectrum is provided in Figure 1B. The two spectra are similar, with only minor chemical shift differences for residues in the regulatory domain of cTnC. Most of these differences occur in residues that are perturbed upon titration of cTnC/cTnI(1−80) with cTnI-(129−166). Several examples will be discussed in detail below.

To identify the cTnC interaction site for cTnI residues 129−166, composite amide chemical shifts of [^{15}N,^{2}H]cTnC bound to cTnI(1−80) were compared before and after titration with cTnI(129−166). Composite amide chemical shift differences are plotted by residue in Figure 2A. Chemical shift perturbations greater than one standard deviation above the mean (indicated by the solid line at 0.07 ppm in Figure 2A) were considered statistically significant. Significant chemical shift perturbations upon binding cTnI-(129−166) were observed in inactive Ca^{2+}-binding site I, Ca^{2+}-binding site II, and the hinge regions surrounding residues 40 and 66. Notably, no significant chemical shift changes were observed in the C-domain of cTnC. This is consistent with cTnI(1−80) preventing spurious interactions between cTnI(129−166) and the cTnC C-domain (*17*). The pattern of chemical shift perturbations indicate that cTnI-(129−166) interacts exclusively with the regulatory domain of Ca^{2+}-saturated cTnC bound to cTnI(1−80).

To determine the structural impact of cTnI residues 81−128, chemical shifts for cTnC bound to cTnI(1−80) were compared to those for cTnC bound to cTnI(1−167). Significant chemical shift perturbations within cTnC were identified in the same regions affected by the binding of cTnI(129−166) (Figure 2B). Several key residues, including L29 and E32 (indicated by inverted triangles, Figure 2B), are broadened beyond detection in this complex, suggesting slightly different dynamic properties for the cTnC regulatory domain in this complex. Additional chemical shift perturbations for residues 45, 55, and 57 within the B and C helices and D87 and T93 within the D/E linker region were observed in the cTnC/cTnI(1−167) complex. These additional chemi-

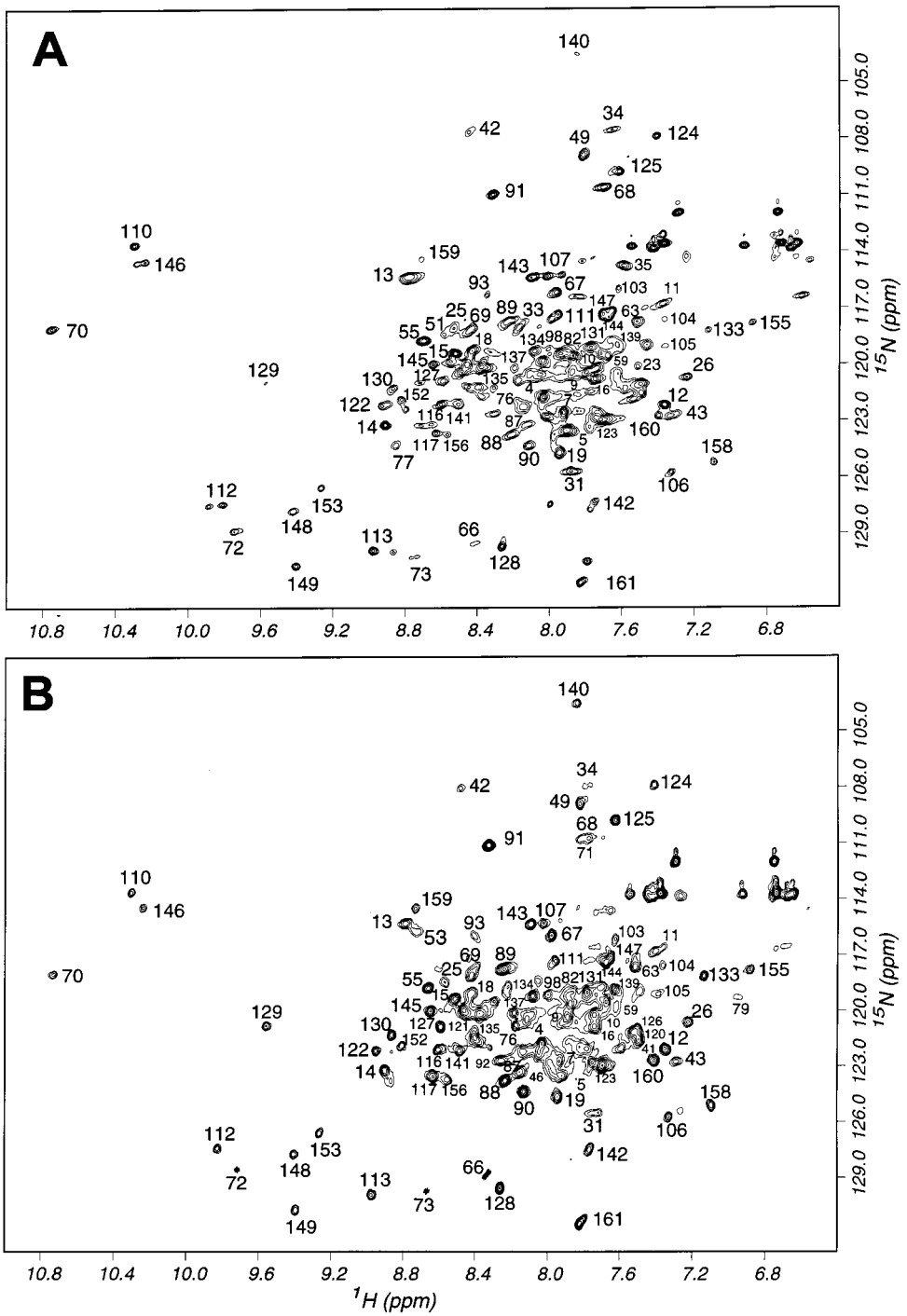

FIGURE 1: ^{1}H−^{15}N Correlation spectra of Ca^{2+}-saturated [^{15}N,^{2}H]cTnC bound to (A) cTnI(1−80) and cTnI(129−166) or (B) cTnI(1−167). Selected cross-peaks are labeled with residue assignments.

cal shift perturbations could result from covalent attachment of the inhibitory region of cTnI to the N-terminus of cTnI or the interaction of cTnI residues 81−128 with cTnC. Tethering of the cTnI regulatory region to the cTnI N-domain may position the cTnI inhibitory region near the D/E linker between the globular N- and C-domains of cTnC. However, Figure 2 demonstrates that the cTnC/cTnI(1−80)/cTnI(129−166) complex derived from two individual segments of cTnI provides a suitable model for the cTnC regulatory domain in the cTnCI complex.

Previous fluorescence resonance energy transfer experiments demonstrated conformational opening of the cTnC regulatory domain upon binding cTnI(129−166) (*9*). A specific pattern of cTnC regulatory domain chemical shift changes can now be correlated with this conformational change. Residues A22, A23, D25, L29, A31, E32, D33, G34, and S35 within the cTnC A-helix and inactive Ca^{2+}-binding loop I and residues E66, G68, S69, T71, V72, and D73 within Ca^{2+}-binding site II demonstrated distinct chemical shift changes through the titration of Ca^{2+}-saturated [^{15}N,^{2}H]cTnC/cTnI(1−80) with cTnI(129−166). For example, the resonance corresponding to A31 moved downfield in the ^{1}H dimension during titration of [^{15}N,^{2}H]cTnC/cTnI(1−80) with cTnI(129−166). Similarly, the resonance corresponding to

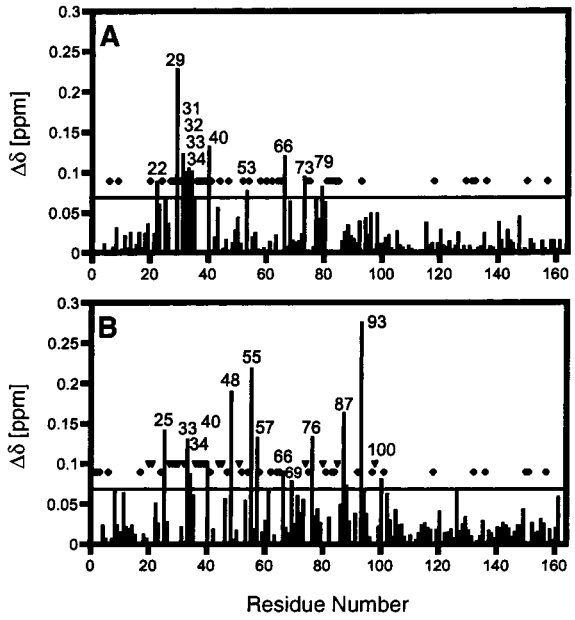

FIGURE 2: Composite absolute value amide chemical shift differences between Ca^{2+}-saturated [^{15}N,^{2}H]cTnC bound to cTnI(1−80) and (A) Ca^{2+}-saturated [^{15}N,^{2}H]cTnC bound to cTnI(1−80) and cTnI(129−166) or (B) Ca^{2+}-saturated [^{15}N,^{2}H]cTnC bound to cTnI(1−167). In panel A, data for residues 1−3, 6, 20, 24, 27, 28, 30, 41, 44, 47, 58, 62, 64, 65, 74, 75, 81−85, 93, 97, 101, 118, 129, 131, 132, 136, 150, and 157 are not available in one or both of the spectra. Residues 36−39 are broadened beyond detection in the presence of cTnI(1−80). Residues 52 and 54 are prolines. Residues for which data are unavailable are marked with filled diamonds. In panel B, data for residues 1−3, 6, 24, 47, 58, 62, 64, 65, 75, 83−85, 97, 101, 118, 132, 136, 150, 151, and 157 are not available in one or both spectra (indicated by filled diamonds). Residues 20, 21, 27−30, 32, 36−39, 44, 45, 51, 57, 74, 80, 85, and 98 (indicated by inverted triangles) were broadened beyond detection in spectra of cTnC bound to cTnI(1−167). In each panel, the horizontal bar indicates one standard deviation above the average composite amide chemical shift difference.

D73 shifted downfield in both ^{1}H and ^{15}N dimensions. Since cTnI(129−166) is known to induce a more open conformation of the regulatory domain of intact cTnC (*9*), these shifts must correlate with an opening of the cTnC regulatory domain. Similar patterns for A31 and D73 were observed previously due to interaction with the unphosphorylated cardiac-specific N-terminus of cTnI and the regulatory domain of cTnC (*12*). The magnitude of the observed chemical shift changes of two relatively isolated resonances G34, in inactive Ca^{2+}-binding loop I, and E66, the terminal residue of helix C preceding Ca^{2+}-binding loop II, are illustrated in Figures 3 and 4, respectively. The corresponding plots from spectra of cTnC bound to cTnI(1−167) are included for comparison.

During the titration of the cTnC/cTnI(1−80) complex with cTnI(129−166), multiple cross-peaks were observed for residue G34, suggesting slow to intermediate exchange for this residue (Figures 1A and 3A). An upfield shift for the G34 cross-peaks in both ^{1}H and ^{15}N dimensions was observed upon cTnI(129−166) binding (Figure 3B,C). In the presence of excess peptide, resonances for G34 coalesce into a single broad resonance with upfield ^{1}H and ^{15}N chemical shifts of 0.1 and 0.3 ppm, respectively, characteristic for the cTnI(129−166)-bound species (Figure 3C). The multiple resonances for G34 in the [^{15}N,^{2}H]cTnC/ cTnI(1−167) complex

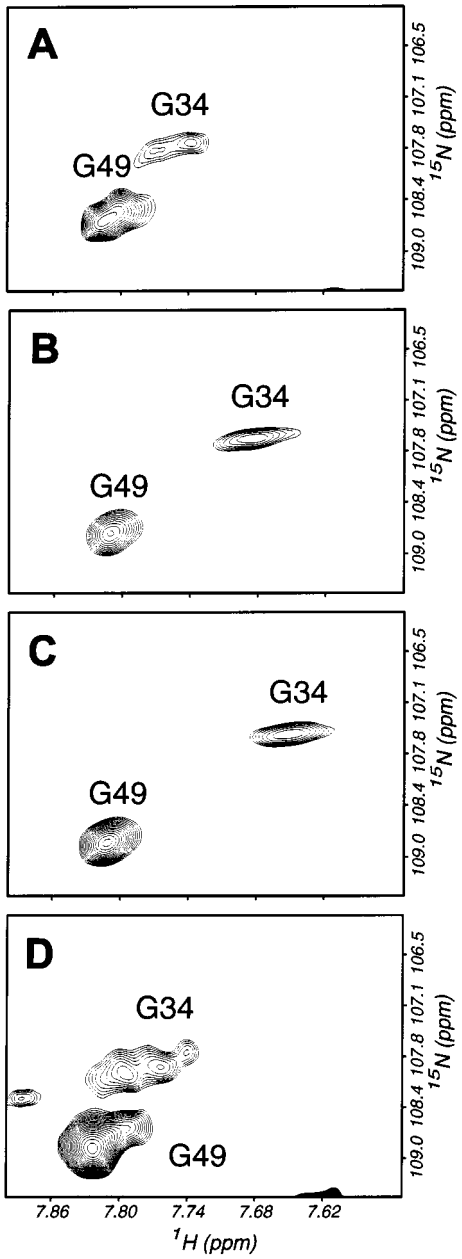

FIGURE 3: Chemical shift changes induced by binding of cTnI(129−166) to the cTnC regulatory domain. Sections of $^{1}H-^{15}N$ correlation spectra showing the resonance(s) for G34 in the Ca^{2+}-saturated [^{15}N,^{2}H]cTnC/cTnI(1−80) complex (A), the Ca^{2+}-saturated [^{15}N,^{2}H]cTnC/cTnI(1−80)/cTnI(129−166) at a 1:1:1.1 ratio (B), the Ca^{2+}-saturated [^{15}N,^{2}H]cTnC/cTnI(1−80)/cTnI(129−166) at a 1:1:2 ratio (C), and the Ca^{2+}-saturated [^{15}N,^{2}H]cTnC/cTnI(1−167) complex (D).

showed only a small upfield shift relative to [^{15}N,^{2}H]cTnC/cTnI(1−80) (Figure 3A,D). The upfield shift corresponding to G34 upon cTnI(129−166) binding correlates with opening of the cTnC regulatory domain. The smaller chemical shift change observed for G34 in the cTnC/cTnI(1−167) complex is consistent with a smaller shift in the conformational equilibrium toward the open state in this complex.

Residue E66 showed multiple broad cross-peaks in spectra of cTnC bound to cTnI(1−80). Addition of cTnI(129−166) resulted in downfield shifts in both ^{1}H and ^{15}N dimensions (Figure 4). Similar to G34, in the presence of excess peptide the cross-peak corresponding to E66 exhibited its maximal

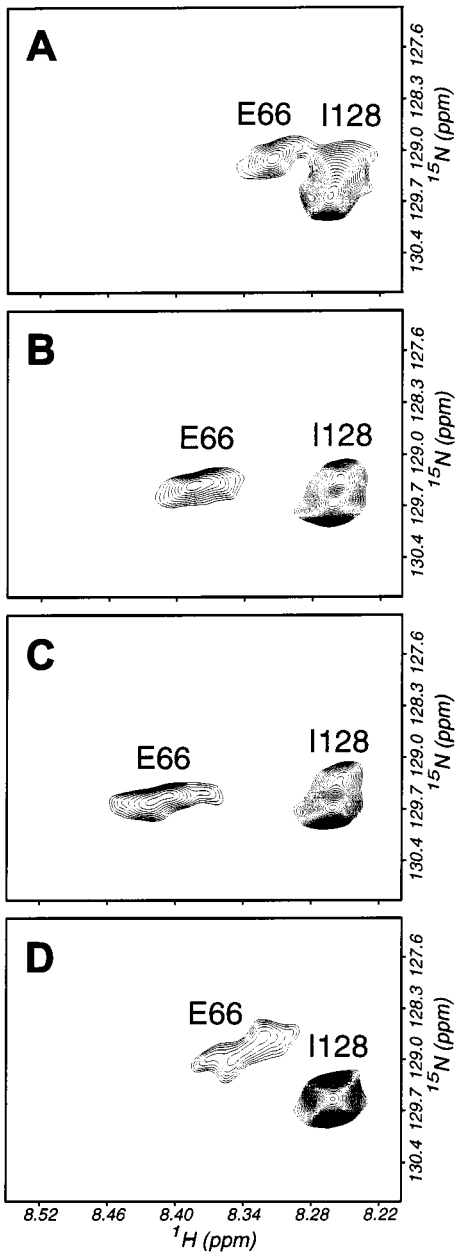

FIGURE 4: Chemical shift changes induced by binding of cTnI(129−166) to the cTnC regulatory domain. Sections of ^{1}H−^{15}N correlation spectra showing the resonance(s) for E66 in the Ca^{2+}-saturated [^{15}N,^{2}H]cTnC/cTnI(1−80) complex (A), the Ca^{2+}-saturated [^{15}N,^{2}H]cTnC/cTnI(1−80)/cTnI(129−166) complex at a ratio of 1:1:1.1 (B), the Ca^{2+}-saturated [^{15}N,^{2}H]cTnC/cTnI(1−80)/cTnI(129−166) complex at a ratio of 1:1:2 (C), and the Ca^{2+}-saturated [^{15}N,^{2}H]cTnC/cTnI(1−167) complex (D).

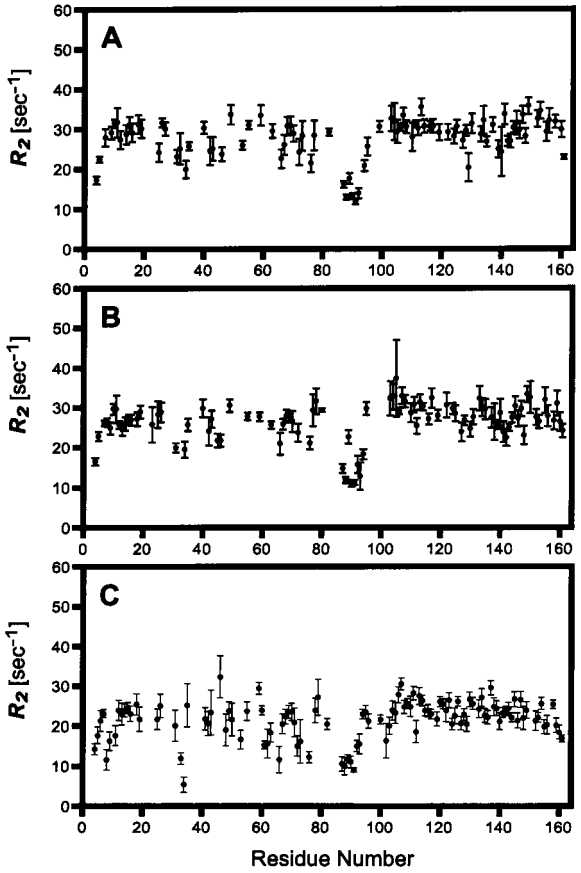

FIGURE 5: ^{15}N Transverse relaxation rates for Ca^{2+}-saturated [^{15}N,^{2}H]cTnC bound to (A) cTnI(1−80) plus 1.1 equiv of cTnI(129−166), (B) cTnI(1−80) plus 2.0 equiv of cTnI(129−166), and (C) cTnI(1−167). (A) Residues 8, 13, 17, 21−24, 29, 33, 45, 50, 51, 56, 57, 60, 61, 78, 80, 86, 93, 96, 98, 100, 109, 115, 120, 121, 123, 126, 138, 151, 154, and 159 were excluded due to spectral overlap or extreme broadening. (B) Residues 17, 21, 22, 33, 48, 50, 53, 56−58, 86, 96, 98, 100, 109, 115, 120, 121, 123, 126, and 154 were excluded due to spectral overlap or extreme broadening. (C) Residues 10, 17, 22, 23, 40, 56, 57, 77, 86, 97, and 99 were excluded due to spectral overlap or broadening.

shift but remained broad (Figure 4C). The resonance for E66 in the cTnC/cTnI(1−167) complex exhibited an intermediate position between that observed for cTnC bound to cTnI(1−80) and the final position reached after addition of a saturating concentration of cTnI(129−166) (Figure 4C).

The observation of multiple cross-peaks for residues G34 and E66 for cTnC bound to cTnI(1−80) is consistent with conformational exchange in the regulatory domain of cTnC. The binding of cTnI(129−166) to the cTnC regulatory domain in the cTnC/cTnI(1−80) complex appeared to shift this equilibrium toward a single predominant conformation. This conformation was shown to represent a more open conformation based on intersite distances obtained in FRET experiments (*9*). Thus saturation of the cTnC regulatory domain with the cTnI(129−166) peptide could force the dynamic equilibrium of the Ca^{2+}-saturated regulatory domain toward the open state. Intermediate positions for cross-peaks of these key residues in cTnC bound to cTnI(1−167) indicate that in this complex, where no excess cTnI was present, an exchange between open and closed conformers persisted. Modulation of this exchange is clearly affected by presence of residues 81−128 between the cTnI regulatory region and the cTnI N-domain in the cTnI(1−167) molecule. The observed conformational exchange may be a functionally significant property of the cardiac troponin complex.

To further investigate the dynamic consequences of cTnI(129−166) interaction with the cTnC regulatory domain in the presence of cTnI(1−80), ^{15}N transverse relaxation rates (R_2) were collected at a proton frequency of 800 MHz on samples with stoichiometric ratios of 1:1:1 (Figure 5A) and 1:1:2 (Figure 5B) for [^{15}N,^{2}H]cTnC/cTnI(1−80)/cTnI(129−166). Based on K_d values obtained by fluorescence (see below), these ratios corresponded to 80% and 96% saturation of the cTnC regulatory domain with cTnI(129−166), re-

spectively. ^{15}N transverse relaxation rates depend on the rotational correlation time of the molecule, dipolar and CSA relaxation phenomena, rapid internal motions, and chemical exchange contributions. The rotational correlation time of the molecule is reflected in the average R_2 value for a domain. Qualitatively, rapid internal motions in the picosecond to nanosecond regime result in depressed R_2 values relative to the domain average, while millisecond time scale motions, typically attributed to chemical exchange, result in elevated R_2 values relative to the domain average. The average ^{15}N R_2 value for both the regulatory domain and the C-domain of cTnC was $\sim$29 s^{-1} (Figure 5). This value was consistent with the molecular mass of cTnC/cTnI(1−80)/cTnI(129−166) and suggested that the two domains tumble together as a unit. Significantly depressed rates in the linker region, residues 84−94, indicated the presence of rapid internal motions and flexibility in this region.

In previous studies utilizing the cTnC/cTnI(1−80) complex and the inhibitory peptide, corresponding to cTnI(129−147), ^{15}N transverse relaxation rates revealed additional interactions between the inhibitory peptide and the cTnC linker region in the presence of excess inhibitory peptide. Since cTnI residues 147−166 interact with the cTnC N-domain, we anticipated that residues 129−147 of the cTnI(129−166) peptide would interact at or near the cTnC D/E linker. Interestingly, no D/E linker interactions were observed at a stoichiometric amount of cTnI(129−166). To rule out interactions between the cTnC D/E linker and the cTnI(129−166) peptide, ^{15}N transverse relaxation rates were also measured in the presence of excess cTnI(129−166) (Figure 5B). Average R_2 values for the two domains were similar to those obtained without excess cTnI(129−166) (Figure 5A). In contrast to the studies utilizing only the cTnI inhibitory peptide (*17*), excess cTnI(129−166) did not result in increased R_2 values for the D/E linker residues of cTnC. These results suggested that the cTnI(129−166) peptide does not interact with the C-domain of cTnC in the presence of cTnI(1−80), nor does it interact appreciably with the linker region of cTnC. Based on ^{15}N transverse relaxation rates and chemical shift mapping, the cTnI(129−166) peptide interacts exclusively with the regulatory domain of cTnC when cTnC is bound to cTnI(1−80). In the context of this peptide, the inhibitory region of cTnI, corresponding to residues 129−147 of cTnI(129−166), appears not to interact substantially with either the D/E linker region or the C-domain of cTnC.

To probe the dynamic consequences of cTnI residues 81−128 and the covalent linkage between the N-domain and the inhibitory and regulatory regions of cTnI, ^{15}N transverse relaxation rates for [^{15}N,^{2}H]cTnC bound to cTnI(1−167) were collected at 800 MHz. Average ^{15}N transverse relaxation rates for each domain were similar, suggesting tumbling of the complex as a single unit (Figure 5C). The average ^{15}N transverse relaxation rate for this complex was also similar to the average rate observed for cTnC bound to cTnI(1−80) and cTnI(129−166) (Figure 5). Resonances corresponding to D33 and G34 within the regulatory domain exhibited lower than average ^{15}N transverse relaxation rates that may indicate rapid internal motions near inactive Ca^{2+}-binding site I. Other residues comprising inactive Ca^{2+} binding site I were in slow conformational exchange, as indicated by multiple cross-peaks in $^{1}H-^{15}N$ correlation spectra of the complex (Figures 1B, 3D, and 4D). Interestingly, linker region flexibility was not reduced upon binding cTnI(1−167), as was observed in the presence of intact cTnI (*12*). This difference in dynamic behavior of the cTnC D/E linker suggests potential cTnC interaction sites within cTnI residues 168−211. This region of cTnI has been previously implicated in cTnC interactions (*16*, *30*). Studies of C-terminal cTnI truncation mutants indicate that cTnI residues 152−199 are essential for Ca^{2+} regulation of myofibrillar ATPase activity (*30*). Ferrières et al. (*16*) identified interactions between cTnI residues 161−178 and 191−210 and cTnC, supporting the hypothesis that cTnC interaction sites exist within the C-terminus of cTnI. However, the structural role of cTnI residues 167−211 in cTnC/cTnI interactions remains to be defined.

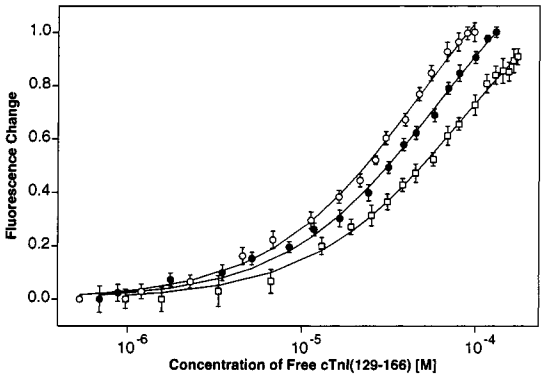

FIGURE 6: Titration of cTnC(F20W/N51C)$_{AEDANS}$ with cTnI(129−166) peptide in the absence or the presence of cTnI(1−80) fragment. The change in tryptophan fluorescence intensity is plotted against the logarithm of free cTnI(129−166) peptide concentration. (○) In the presence of 20 μM cTnI(1−80); (●) in the presence of 20 μM cTnI(1−80)pp; (□) no cTnI(1−80). The solid curves were the best fitted results obtained from eq 2 (see text). Error bars are deviations from two measurements. Excitation wavelength was 295 nm and emission was detected at 331 nm.

Phosphorylation of the cardiac-specific N-terminus of cTnI by PKA reduces the apparent Ca^{2+} affinity of the lone active Ca^{2+}-binding site II (*20*). We predicted that phosphorylation of cTnI(1−80) bound to cTnC would affect the strength of interactions between cTnI(129−166) and the regulatory domain of cTnC. Fluorescence emission from cTnC(F20W/N51C)$_{AEDANS}$ is sensitive to cTnI(129−166) binding at the cTnC regulatory domain and was used to monitor the interaction between cTnI(129−166) and the regulatory domain of cTnC, in the presence of cTnI(1−80) or PKA-phosphorylated cTnI(1−80) and in the absence of cTnI(1−80). Representative binding curves are shown in Figure 6.

The data were fit as described under Experimental Procedures to determine the K_d for each sample. Solid curves represent typical fits, from which dissociation constants were determined. The highest K_d, 86.8 ± 3.0 μM, was obtained for cTnC titrated with cTnI(129−166). With cTnI(1−80) bound to the C-domain of cTnC, the K_d for cTnI(129−166) was 43.4 ± 3.2 μM. The apparent weaker affinity of cTnC for cTnI(129−166) in the absence of cTnI(1−80) is likely due to ancillary binding of the peptide to the cTnC C-domain hydrophobic pocket. This competing binding site is eliminated in the presence of cTnI(1−80). Phosphorylation of cTnI(1−80) by PKA reduced the affinity of cTnC for cTnI(129−166), yielding a K_d of 59.1 ± 1.3 μM. Error analysis suggested that the major source of uncertainty in K_d values

arose from the data at low cTnI(129−166) concentrations. At higher concentrations of the peptide the two binding curves for cTnI(129−166) in the presence and absence of cTnI(1−80) PKA phosphorylation were well separated. This suggests that the dissociation constants of 43.4 and 59.1 μM reflect different affinities for cTnI(129−166) as a consequence of cTnI phosphorylation. Student's *t*-test returned a *P* value of 0.025 for phosphorylated versus nonphosphorylated cTnI(1−80), which is indicative of a statistically significant difference between the two K_d values. The magnitude of this difference may be amplified or diminished in the context of the intact cTnI molecule or in the thin filament within the contractile apparatus of the myocyte. The demonstration of the effect of cTnI phosphorylation on the cTnC regulatory domain function in the absence of an intact cTnI molecule indicates that propagation of at least a portion of this signal through cTnI is not required. While the cardiac-specific N-terminus of cTnI interacts directly with the cTnC regulatory domain, and PKA phosphorylation affects this interaction directly, these results do not exclude the possibility of additional effects of PKA phosphorylation propagated through intact cTnI to the regulatory domain of cTnC that cannot be appreciated in this study (*10, 12*).

Taken together, the data provide an interesting picture of the interactions between cTnC and the various regions of cTnI. Chemical shift perturbations mapped cTnI(129−166) interactions to the cTnC regulatory domain. ^{15}N Transverse relaxation rates indicated that cTnI(129−166) alters the dynamics of the regulatory domain but does not reduce the flexibility of the cTnC linker region. This is in contrast to either full-length cTnI or saturating amounts of cTnI(129−147), both of which appeared to restrict linker region mobility (*12, 17*). Comparison of chemical shifts and ^{15}N transverse relaxation rates for cTnC/cTnI(1−80)/cTnI(129−166) and cTnC/cTnI(1−167) suggest the cTnI residues 81−129 do not strongly interact with cTnC but may modulate the interaction of the cTnI regulatory region with the cTnC regulatory domain. Dissociation constants determined by fluorescence emission revealed that phosphorylation of cTnI(1−80) reduced the apparent affinity of the regulatory domain of cTnC for cTnI(129−166). These results provide insight into the structural interactions within the cTnC/cTnI complex and the mechanism of PKA modulation of Ca^{2+} sensitivity of muscle contraction.

DISCUSSION

Despite years of intense investigation, structural details of the cardiac troponin switch mechanism remain elusive. Ca^{2+}- and/or Mg^{2+}-dependent structural interactions between the N-domain of cTnI and the C-domain of cTnC have been demonstrated by both crystallographic and solution NMR techniques (*31, 32*). These interactions likely account for the stability of the cTnC/cTnI interaction in the relaxation phase of muscle contraction when the intracellular Ca^{2+} concentration is low. An additional cTnC interaction site, corresponding to residues 147−166, has been identified within cTnI (*4*). A synthetic peptide based on this sequence interacts with the isolated cTnC regulatory domain in a Ca^{2+}-dependent manner (*4*). This interaction is thought to play a key role in the Ca^{2+}-activated switch. It has long been presumed that the adjacent inhibitory region of cTnI, which binds actin to inhibit muscle contraction, binds cTnC in a Ca^{2+}-dependent manner. Many peptide-based experiments have demonstrated interactions between this region of cTnI, corresponding to residues 129−147, and both globular domains and the linker region of cTnC (*27, 29, 33*−*39*). Chemical cross-linking experiments, utilizing intact TnC and TnI molecules, have also produced disparate results for the TnC binding site of the TnI inhibitory region depending on the conditions and reagents used (*40*−*44*).

In the presence of cTnI(1−80), a peptide corresponding to the cTnI inhibitory region, cTnI(129−147), was shown not to interact with the C-domain of cTnC (*17*). However, weak interaction could be detected with the regulatory domain and linker region of cTnC (*17*). The chemical shift changes observed upon binding of cTnI(129−166) to cTnC in the presence of cTnI(1−80) are much larger than those previously observed upon binding the cTnI(129−147) peptide. This difference is attributable to the presence of cTnI residues 147−166, which bind to the cTnC regulatory domain hydrophobic pocket and shift the conformational equilibrium toward the open or active state (*9*). Surprisingly, ^{15}N transverse relaxation rates and chemical shift perturbations did not reveal any interactions between cTnI(129−166) and the linker region of cTnC, even in the presence of a 2-fold excess of cTnI(129−166). This result indicates that the inhibitory region may not specifically interact with cTnC in the presence of Ca^{2+} or that specific interactions require covalent linkage of the inhibitory region of cTnI to the N-terminal region of cTnI. The lack of linker region restriction indicated by the ^{15}N transverse relaxation rates for cTnC bound to cTnI(1−167) favors the first conclusion.

Recent studies on the skeletal TnC/TnI complex have shown that the available structural data is consistent with the cTnI inhibitory region localized near the linker region of cTnC (*45*). In the presence of Ca^{2+}, the TnI inhibitory region would be pulled away from actin by interaction of the TnI regulatory region with the N-domain of TnC. This model is consistent with our data showing little or no interaction of the cTnI inhibitory region residues 129−147 with cTnC and interaction of residues 148−166 with the cTnC regulatory domain hydrophobic cleft. Positioning of the cTnI regulatory region within the cTnC regulatory domain hydrophobic cleft could place the cTnI inhibitory region near the D/E linker (*45*).

Correlation of specific cTnC regulatory domain chemical shift changes upon binding cTnI(129−166) with conformational opening of the cTnC regulatory domain monitored by FRET measurements provides a powerful tool for analysis of the cTnC/cTnI Ca^{2+}-activated switch mechanism. Previous studies have suggested that the cardiac-specific N-terminus of cTnI shifts the conformational equilibrium of the Ca^{2+}-saturated cTnC regulatory domain toward the open state. The similarities in the pattern of chemical shift changes observed here to those previously observed would support this conclusion (*12*). Stabilization of the Ca^{2+}-saturated cTnC regulatory domain open conformation would be the anticipated structural activity of a Ca^{2+} sensitizing agent. The ability to identify opening of the cTnC regulatory domain in the intact cTnC/cTnI complex could be utilized to identify and refine compounds that not only interact with cTnC but also exhibit the desired physiological activity.

The cTnC/cTnI(1−80)/cTnI(129−166) complex allowed dissection of the PKA Ca^{2+}-sensitivity modulation mecha-

nism. Fluorescence measurements demonstrating a statistically significant decrease in affinity between cTnC and cTnI(129−166) provide the first structural insight into propagation of the phosphorylation signal beyond altered Ca^{2+}-binding affinity. This result indicates that PKA phosphorylation of the cTnI cardiac-specific N-terminus alters the strength of Ca^{2+}-dependent regulatory interactions between cTnC and cTnI. The small magnitude of the difference may be sufficient to alter the Ca^{2+} sensitivity of muscle contraction due to the high degree of cooperativity with the thin filament regulatory apparatus. Potential effects of PKA phosphorylation of cTnI propagated through cTnI to the cTnC/cTnI regulatory interactions could not be identified in this study but could add to the effect of direct interactions between the cardiac-specific N-terminus of cTnI and the Ca^{2+}-saturated cTnC regulatory domain.

Two opposing models have been proposed for β-adrenergic modulation of Ca^{2+} sensitivity of muscle contraction. The direct interaction model suggests that the cardiac-specific N-terminus of cTnI interacts directly with Ca^{2+}-saturated cTnC regulatory domain to stabilize the open or active conformation. PKA phosphorylation of the cardiac-specific N-terminus of cTnI eliminates these interactions, decreasing Ca^{2+}-binding affinity at the cTnC regulatory site (*10*, *12*). The indirect transmission model postulates that phosphorylation at the cTnI N-terminus induces a global change in cTnI structure, which indirectly alters cTnC Ca^{2+} sensitivity (*46*). The effect of cTnI phosphorylation on cTnC/cTnI regulatory interactions in the absence of any physical linkage between the cTnI N-terminus and the cTnI regulatory region lends support to the direct interaction model. However, it does not eliminate the possibility of contributions from indirect propagation of the PKA signal through cTnI. The full effect of PKA phosphorylation may only be realized in the context of the intact contractile apparatus. While these results favor the direct model over the indirect model, the actual mechanism remains to be more fully defined. The two models provide a basis for further experimentation and must be refined to accommodate the results of future experiments.

On the basis of results presented here and in the literature, the model for troponin regulation of cardiac muscle contraction can be further refined. Residues 33−70 of cTnI provide a structural link between cTnC and cTnI. The inhibitory region of cTnI, consisting of residues 129−147, does not interact specifically with cTnC in a single interaction. The regulatory region of cTnI, consisting of residues 147−166, interacts with the regulatory domain of cTnC in a Ca^{2+}-dependent manner, controlling the interaction between the inhibitory region of cTnI and actin. The cardiac-specific N-terminus serves to modify the Ca^{2+} sensitivity of the troponin switch upon phosphorylation by PKA. Phosphorylation of the cardiac-specific N-terminus of cTnI removes interactions with the regulatory domain of cTnC. Thus, the phosphorylation signal is propagated from the cardiac-specific N-terminus of cTnI through the regulatory domain of cTnC to the regulatory region of cTnI. This model is consistent with the majority of the available data and provides a foundation for further experimentation.

ACKNOWLEDGMENT

We thank Drs. Jill Trewhella and Michael Wall for communication of their cardiac TnC/TnI model prior to publication (*45*). We also thank Natosha Finley for expression and purification of [^{15}N,^{2}H]cTnC protein.

REFERENCES

1. Kobayashi, T., Kobayashi, M., Gryczynski, Z., Lakowicz, J. R., and Collins, J. H. (2000) *Biochemistry 39*, 86−91.
2. Herzberg, O., and James, M. N. (1985) *Nature 313*, 653−9.
3. Holroyde, M. J., Robertson, S. P., Johnson, J. D., Solaro, R. J., and Potter, J. D. (1980) *J. Biol. Chem. 255*, 11688−93.
4. Li, M. X., Spyracopoulos, L., and Sykes, B. D. (1999) *Biochemistry 38*, 8289−98.
5. Gagne, S. M., Tsuda, S., Li, M. X., Smillie, L. B., and Sykes, B. D. (1995) *Nat. Struct. Biol. 2*, 784−9.
6. Spyracopoulos, L., Li, M. X., Sia, S. K., Gagne, S. M., Chandra, M., Solaro, R. J., and Sykes, B. D. (1997) *Biochemistry 36*, 12138−46.
7. Strynadka, N. C., Cherney, M., Sielecki, A. R., Li, M. X., Smillie, L. B., and James, M. N. (1997) *J. Mol. Biol. 273*, 238−55.
8. Gagne, S. M., Tsuda, S., Li, M. X., Chandra, M., Smillie, L. B., and Sykes, B. D. (1994) *Protein Sci. 3*, 1961−74.
9. Dong, W. J., Xing, J., Villain, M., Hellinger, M., Robinson, J. M., Chandra, M., Solaro, R. J., Umeda, P. K., and Cheung, H. C. (1999) *J. Biol. Chem. 274*, 31382−90.
10. Gaponenko, V., Abusamhadneh, E., Abbott, M. B., Finley, N., Gasmi-Seabrook, G., Solaro, R. J., Rance, M., and Rosevear, P. R. (1999) *J. Biol. Chem. 274*, 16681−4.
11. Paakkonen, K., Annila, A., Sorsa, T., Pollesello, P., Tilgmann, C., Kilpelainen, I., Karisola, P., Ulmanen, I., and Drakenberg, T. (1998) *J. Biol. Chem. 273*, 15633−8.
12. Abbott, M. B., Gaponenko, V., Abusamhadneh, E., Finley, N., Li, G., Dvoretsky, A., Rance, M., Solaro, R. J., and Rosevear, P. R. (2000) *J. Biol. Chem. 275*, 20610−20617.
13. Finley, N., Dvoretsky, A., and Rosevear, P. R. (2000) *J. Mol. Cell. Cardiol. 32*, 1439−46.
14. Calvert, M. J., Ward, D. G., Trayer, H. R., and Trayer, I. P. (2000) *J. Biol. Chem. 275*, 32508−15.
15. Krudy, G. A., Kleerekoper, Q., Guo, X., Howarth, J. W., Solaro, R. J., and Rosevear, P. R. (1994) *J. Biol. Chem. 269*, 23731−5.
16. Ferrieres, G., Pugniere, M., Mani, J. C., Villard, S., Laprade, M., Doutre, P., Pau, B., and Granier, C. (2000) *FEBS Lett. 479*, 99−105.
17. Abbott, M. B., Dvoretsky, A., Gaponenko, V., and Rosevear, P. R. (2000) *FEBS Lett. 469*, 168−72.
18. Farah, C. S., and Reinach, F. C. (1995) *FASEB J. 9*, 755−67.
19. Stefancsik, R., Jha, P. K., and Sarkar, S. (1998) *Proc. Natl. Acad. Sci. U.S.A. 95*, 957−62.
20. Robertson, S. P., Johnson, J. D., Holroyde, M. J., Kranias, E. G., Potter, J. D., and Solaro, R. J. (1982) *J. Biol. Chem. 257*, 260−3.
21. Zhang, R., Zhao, J., Mandveno, A., and Potter, J. D. (1995) *Circ. Res. 76*, 1028−35.
22. Dohet, C., al-Hillawi, E., Trayer, I. P., and Ruegg, J. C. (1995) *FEBS Lett. 377*, 131−4.
23. Finley, N., Abbott, M. B., Abusamhadneh, E., Gaponenko, V., Dong, W., Gasmi-Seabrook, G., Howarth, J. W., Rance, M., Solaro, R. J., Cheung, H. C., and Rosevear, P. R. (1999) *FEBS Lett. 453*, 107−12.
24. Dong, W. J., Xing, J., Chandra, M., Solaro, J., and Cheung, H. C. (2000) *Proteins: Struct., Funct., Genet. 41*, 438−47.
25. Kay, L. E., Keifer, P., and Saarinen, T. (1992) *J. Am. Chem. Soc. 114*, 10663−10665.
26. Zhang, O., Kay, L. E., Olivier, J. P., and Forman-Kay, J. D. (1994) *J. Biomol. NMR 4*, 845−58.
27. Howarth, J. W., Krudy, G. A., Lin, X., Putkey, J. A., and Rosevear, P. R. (1995) *Protein Sci. 4*, 671−80.
28. Campbell, A. P., Van Eyk, J. E., Hodges, R. S., and Sykes, B. D. (1992) *Biochim. Biophys. Acta 1160*, 35−54.
29. Li, M. X., Spyracopoulos, L., Beier, N., Putkey, J. A., and Sykes, B. D. (2000) *Biochemistry 39*, 8782−90.

30. Rarick, H. M., Tu, X. H., Solaro, R. J., and Martin, A. F. (1997) *J. Biol. Chem. 272*, 26887−92.
31. Vassylyev, D. G., Takeda, S., Wakatsuki, S., Maeda, K., and Maeda, Y. (1998) *Proc. Natl. Acad. Sci. U.S.A. 95*, 4847−52.
32. Gasmi-Seabrook, G. M., Howarth, J. W., Finley, N., Abusamhadneh, E., Gaponenko, V., Brito, R. M., Solaro, R. J., and Rosevear, P. R. (1999) *Biochemistry 38*, 8313−22.
33. Pearlstone, J. R., and Smillie, L. B. (1995) *Biochemistry 34*, 6932−40.
34. McKay, R. T., Tripet, B. P., Hodges, R. S., and Sykes, B. D. (1997) *J. Biol. Chem. 272*, 28494−500.
35. Tripet, B., Van Eyk, J. E., and Hodges, R. S. (1997) *J. Mol. Biol. 271*, 728−50.
36. Pearlstone, J. R., Sykes, B. D., and Smillie, L. B. (1997) *Biochemistry 36*, 7601−6.
37. Kobayashi, T., Leavis, P. C., and Collins, J. H. (1996) *Biochim. Biophys. Acta 1294*, 25−30.
38. Grabarek, Z., Drabikowski, W., Leavis, P. C., Rosenfeld, S. S., and Gergely, J. (1981) *J. Biol. Chem. 256*, 13121−7.
39. Jha, P. K., Mao, C., and Sarkar, S. (1996) *Biochemistry 35*, 11026−35.
40. Kobayashi, T., Tao, T., Gergely, J., and Collins, J. H. (1994) *J. Biol. Chem/ 269*, 5725−9.
41. Kobayashi, T., Zhao, X., Wade, R., and Collins, J. H. (1999) *Biochim. Biophys. Acta 1430*, 214−21.
42. Grabarek, Z., Mabuchi, Y., and Gergely, J. (1990) *Adv. Exp. Med. Biol. 269*, 85−8.
43. Ngai, S. M., Sonnichsen, F. D., and Hodges, R. S. (1994) *J. Biol. Chem. 269*, 2165−72.
44. Luo, Y., Leszyk, J., Qian, Y., Gergely, J., and Tao, T. (1999) *Biochemistry 38*, 6678−88.
45. Tung, C. S., Wall, M. E., Gallagher, S. C., and Trewhella, J. (2000) *Protein Sci. 9*, 1312−26.
46. Chandra, M., Dong, W. J., Pan, B. S., Cheung, H. C., and Solaro, R. J. (1997) *Biochemistry 36*, 13305−11.

BI0100642